

Biodistribution, Pharmacokinetics, and Dosimetry of ^{177}Lu -, ^{90}Y -, and ^{111}In -Labeled Somatostatin Receptor Antagonist OPS201 in Comparison to the Agonist ^{177}Lu -DOTATATE: The Mass Effect

Guillaume P. Nicolas^{1,2}, Rosalba Mansi³, Lisa McDougall^{1,3}, Jens Kaufmann⁴, Hakim Bouterfa⁴, Damian Wild^{1,2}, and Melpomeni Fani^{1,3}

¹Division of Nuclear Medicine, University Hospital of Basel, Basel, Switzerland; ²Center for Neuroendocrine and Endocrine Tumors, University Hospital of Basel, Basel, Switzerland; ³Division of Radiopharmaceutical Chemistry, University Hospital of Basel, Basel, Switzerland; and ⁴OctreoPharm Sciences GmbH, Ipsen Group, Berlin, Germany

Radiolabeled somatostatin receptor (SSTR) antagonists have shown in vivo higher uptake in SSTR-expressing tumors than agonists. In this preclinical study, the SSTR2 antagonist OPS201 (DOTA-JR11; DOTA-[Cpa-c(DCys-Aph(Hor)-Daph(Cbm)-Lys-Thr-Cys)-DTyr-NH₂]) labeled with ^{177}Lu , ^{90}Y , and ^{111}In was compared with the SSTR2 agonist ^{177}Lu -DOTATATE. **Methods:** Biodistribution, pharmacokinetics, SPECT/CT, and dosimetry studies were performed to assess the bioequivalence of all radiotracers. Use of escalated peptide mass and nephroprotective agents were systematically investigated. **Results:** The tumor residence time was 15.6 h (13.4–17.7) for ^{177}Lu -OPS201 (10 pmol) and 6.4 h (5.4–7.3) for ^{177}Lu -DOTATATE, resulting in a 2.5-times-higher tumor dose for the antagonist than for the agonist (0.854 vs. 0.333 mGy/MBq for a 4-cm tumor). The overall tumor-to-kidney dose ratio was approximately 24% and 32% higher for ^{177}Lu -OPS201 than for ^{90}Y -OPS201 and ^{177}Lu -DOTATATE, respectively. ^{111}In -OPS201 had a biodistribution significantly different from ^{90}Y -OPS201 and is therefore not a surrogate for ^{90}Y -OPS201 dosimetry studies. Importantly, and in contrast to ^{177}Lu -DOTATATE, injection of 10, 200, and 2,000 pmol of ^{177}Lu -OPS201 did not cause any relevant tumor saturation, with tumor uptake 4 h after injection: 23.9, 24.9, and 18.8 percentage of injected activity per gram of tissue (%IA/g), respectively, for the antagonist ($P > 0.05$), as compared with 17.8, 12.0, and 9.9 %IA/g for the agonist ($P < 0.05$). Increasing the peptide mass of ^{177}Lu -OPS201 from 10 to 200 pmol drastically decreased the effective dose from 0.0908 to 0.0184 mSv/MBq and decreased the uptake in the liver, bone marrow, and all SSTR2-expressing organs; thus, the therapeutic index improved considerably. Lysine and succinylated gelatine, alone or in combination, significantly reduced the renal dose of ^{177}Lu -OPS201 compared with the control group, by 45%, 25%, and 40%, respectively ($P < 0.05$). The reduction was similar for 10 and 200 pmol, whereas lysine performed better than succinylated gelatine. **Conclusion:** ^{177}Lu -OPS201 exhibits higher tumor uptake, longer tumor residence time, and improved tumor-to-kidney dose ratio compared with ^{177}Lu -DOTATATE and ^{90}Y -OPS201. Importantly, the mass-escalation study indicates that an optimized antagonist

mass might further improve the safety window of peptide receptor radionuclide therapy by reducing the liver and bone marrow doses as well as the effective dose. Clinical studies are warranted to confirm the efficacy and advantageous toxicity profile of ^{177}Lu -OPS201.

Key Words: somatostatin receptor antagonists; radionuclide therapy; receptor targeting; ^{177}Lu ; neuroendocrine tumors

J Nucl Med 2017; 58:1435–1441
DOI: 10.2967/jnumed.117.191684

Neuroendocrine tumors (NETs) occur with an incidence of approximately 4 per 100,000 individuals (1,2); they are usually slow growing, which explains their relatively high prevalence of 35/100,000 (1). Because 40%–95% of the patients present with evidence of metastatic spread at diagnosis (3), systemic treatments are often necessary. Somatostatin (sst) receptors, especially the subtype 2 (SSTR2), are widely overexpressed on NET cells, therefore making SSTR2 an excellent molecular target for treatment of NET with somatostatin analogs and peptide receptor radionuclide therapy (PRRT). Current clinical protocols of PRRT use somatostatin agonists labeled with ^{90}Y or ^{177}Lu , such as ^{90}Y -DOTATOC and ^{177}Lu -DOTATATE. These have been shown to relieve symptoms, induce tumor response, and improve progression-free survival (4–7); however, complete remission is rarely achieved (8).

Ginje et al. were the first to show in animal studies that radiolabeled SSTR antagonists, despite the fact that they do not internalize, showed tumor targeting properties superior to those of agonists, most probably because of the larger population of binding sites recognized by the antagonists (9). In SSTR2-expressing human tumor samples, using in vitro receptor autoradiography, the SSTR2 antagonist ^{177}Lu -DOTA-BASS showed a higher accumulation than the SSTR2-agonist ^{177}Lu -DOTATATE (10). These results were confirmed clinically in a pilot imaging study with ^{111}In -DOTA-BASS versus the SSTR2 agonist ^{111}In -pentetreotide (Octreoscan) (11). From a small library of potent SSTR2 antagonists (12), JR11 (satoreotide; [Cpa-c(DCys-Aph(Hor)-Daph(Cbm)-Lys-Thr-Cys)-DTyr-NH₂]) was chosen for a PRRT feasibility study with antagonists. In this pilot study, ^{177}Lu -OPS201 (^{177}Lu -DOTA-JR11) demonstrated a favorable biodistribution profile, compared with ^{177}Lu -DOTATATE, and a 1.7–10.6 higher tumor dose (13). Recently, it was shown that JR11 is particularly attractive for

Received Feb. 10, 2017; revision accepted Apr. 11, 2017.
For correspondence or reprints contact either of the following:
Melpomeni Fani, University Hospital of Basel, Petersgraben 4, 4031 Basel, Switzerland.
E-mail: melpomeni.fani@usb.ch
Damian Wild, University Hospital of Basel, Petersgraben 4, 4031 Basel, Switzerland.
E-mail: damian.wild@usb.ch
Published online Apr. 27, 2017.
COPYRIGHT © 2017 by the Society of Nuclear Medicine and Molecular Imaging.

TABLE 1
Biodistribution of 10 pmol ^{177}Lu -OPS201 and ^{177}Lu -DOTATATE in Nude Mice Bearing HEK-hsstr2 Tumor Xenografts

Organ	4 h	72 h	168 h
^{177}Lu-OPS201			
Blood	0.10 ± 0.02	0.01 ± 0.00	0.00 ± 0.00
Heart	0.61 ± 0.09	0.07 ± 0.01	0.03 ± 0.02
Lung	6.59 ± 3.41	1.32 ± 1.15	0.44 ± 0.32
Liver	1.45 ± 0.33	0.32 ± 0.06	0.23 ± 0.07
Pancreas	47.0 ± 4.20	5.53 ± 1.21	2.06 ± 0.25
Spleen	1.39 ± 0.69	0.32 ± 0.09	0.22 ± 0.02
Stomach	49.8 ± 8.19	9.13 ± 2.14	4.73 ± 0.93
Intestine	9.46 ± 2.24	1.72 ± 0.82	0.48 ± 0.30
Adrenal	8.16 ± 1.72	2.98 ± 0.97	1.19 ± 0.20
Kidney	5.88 ± 0.85	2.18 ± 0.26	0.78 ± 0.06
Muscle	0.10 ± 0.03	0.02 ± 0.01	0.01 ± 0.00
Femur	1.24 ± 0.92	0.73 ± 0.42	0.29 ± 0.23
Salivary gland	2.32 ± 0.47	0.25 ± 0.13	0.15 ± 0.06
Tumor	23.9 ± 4.76	11.7 ± 2.15	2.44 ± 1.17
^{177}Lu-DOTATATE			
Blood	0.07 ± 0.01	0.00 ± 0.00	0.00 ± 0.00
Heart	0.29 ± 0.06	0.07 ± 0.02	0.04 ± 0.01
Lung	6.54 ± 3.49	2.90 ± 1.47	0.77 ± 0.22
Liver	0.26 ± 0.04	0.09 ± 0.02	0.07 ± 0.00
Pancreas	10.3 ± 1.66	0.96 ± 0.20	0.51 ± 0.10
Spleen	0.76 ± 0.18	0.26 ± 0.06	0.12 ± 0.03
Stomach	12.2 ± 2.23	3.23 ± 0.60	1.85 ± 0.85
Intestine	5.80 ± 1.20	1.81 ± 0.35	0.82 ± 0.31
Adrenal	9.27 ± 2.49	3.42 ± 0.78	2.04 ± 0.76
Kidney	5.10 ± 0.94	0.96 ± 0.14	0.43 ± 0.03
Muscle	0.03 ± 0.01	0.00 ± 0.00	0.00 ± 0.00
Femur	1.55 ± 0.36	0.61 ± 0.14	0.47 ± 0.06
Salivary gland	0.68 ± 0.40	0.04 ± 0.01	0.03 ± 0.01
Tumor	17.8 ± 4.35	3.66 ± 0.54	0.86 ± 0.11

Data are %IA/g ± SD, $n = 3-6$.

targeting not only NETs but also other types of tumors that normally express a low density of SSTR2, such as breast carcinomas, renal cell cancers, and others (14).

The use of radiolabeled SSTR antagonists is new and, despite some preliminary human data (11,13), more information is needed to better understand their potential clinical performances and limitations. Also, key properties such as receptor affinity, tumor uptake, and retention (15) of the radiolabeled SSTR2 antagonists, including JR11, may be significantly influenced by the chelator and the radiometal used (16,17). Therefore, in the present study, we addressed issues related to the bioequivalence of ^{177}Lu -, ^{90}Y -, and ^{111}In -labeled OPS201. Pharmacokinetics, biodistribution, and dosimetry were investigated, while studying with particular attention the therapeutic index and other aspects related to clinical translation of this therapeutic compound. In this respect, we

systematically addressed the role of the peptide mass and the use of various clinically available nephroprotective agents. All investigations were compared head to head with ^{177}Lu -DOTATATE in an SSTR2-expressing tumor model.

MATERIALS AND METHODS

Reagents and Cell Lines

OPS201 was kindly supplied by OctreoPharm, DOTATATE was purchased from piChem, and all reagents were from common suppliers.

The human embryonic kidney (HEK) cells, stably transfected with the human SSTR2 (HEK-hsstr2), were kindly provided by Professor Stefan Schulz and cultured as previously described (16,17).

Preparation of Radiotracers

^{177}Lu -DOTATATE, ^{177}Lu -OPS201, ^{90}Y -OPS201, and ^{111}In -OPS201 were prepared in ammonium acetate buffer (0.4 M, pH 5.0) after incubation of 2.5–25 μg of the corresponding conjugate (1 mg/mL) with different activities of $^{177}\text{LuCl}_3$ (ITM), $^{90}\text{YCl}_3$ (PerkinElmer), or $^{111}\text{InCl}_3$ (Mallinckrodt), at 95°C for 30 min. Quality control was performed by reversed-phase high-performance liquid chromatography, as described elsewhere (17). The radiotracer solutions were prepared by dilution with 0.9% NaCl containing 0.05% human serum albumin.

Biodistribution Studies

Animals were housed and cared for according to Swiss regulations on animal experimentation (approval no. 789). Female athymic Nude-Foxn1^{nu} mice, 4–6 wk old, were inoculated subcutaneously in the shoulder with 1×10^7 HEK-hsstr2, freshly suspended in 100 μL of sterile phosphate-buffered saline. Tumors were allowed to grow for 2–3 wk.

Biodistribution studies were performed after intravenous injection, in the tail vein, of 100 μL of the investigated radiotracer. At each time point, a cohort of mice was sacrificed under anesthesia. Blood samples and organs of interest were collected, blotted dry, weighted, and counted in a γ -counter. The results were expressed as mean ± SD and represent the percentage of injected activity per gram of tissue (%IA/g). Nonspecific uptake was determined with a 2- to 5-min preinjection of 20 nmol of the nonlabeled conjugate.

The following investigations were performed: (1) Comparison of the pharmacokinetics of 10 pmol ^{177}Lu -OPS201 with ^{177}Lu -DOTATATE from 1 up to 168 h after injection; study of the influence of the radiometal on the biodistribution of OPS201 (10 pmol) labeled with ^{177}Lu , ^{90}Y , and ^{111}In , 4 and 72 h after injection (^{177}Lu and ^{90}Y were also compared at 24 h). (2) Study of the influence of the peptide amount (10, 200, or 2,000 pmol) on the biodistribution of ^{177}Lu -OPS201 4 h after injection, and comparison with ^{177}Lu -DOTATATE. (3) Study of the

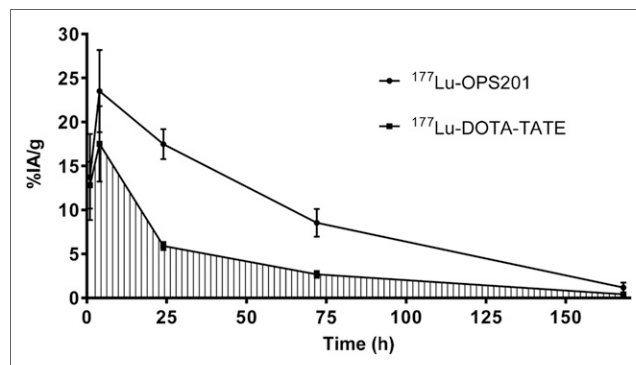


FIGURE 1. Time-activity curve in tumor for ^{177}Lu -OPS201 and for ^{177}Lu -DOTATATE. These pharmacokinetic data were generated from serial independent biodistribution experiments performed 1, 4, 24, 72, and 168 h after injection.

influence of the peptide amount (10 and 200 pmol) on the pharmacokinetics of ^{177}Lu -OPS201 versus ^{177}Lu -DOTATATE from 4 up to 168 h after injection. (4) Study of the best nephroprotective regimen for reducing the kidney dose of ^{177}Lu -OPS201. Lysine (20 mg/100 μL in phosphate-buffered saline) or Gelofusine (succinylated gelatine; B. Braun Medical; 4 mg/100 μL) or a combination of both (20 mg of lysine and 4 mg of Gelofusine/150 μL) were injected 5 min before administration of 10 pmol ^{177}Lu -OPS201 and compared after 4 h. Lysine alone and a combination of lysine plus Gelofusine were also evaluated for 200 pmol ^{177}Lu -OPS201, 4 h after injection.

Dosimetry

Mouse biodistribution data were used to generate time-activity curves for each radiotracer. Because of the absence of a specific radioactivity accumulation in bones and red marrow, a linear relationship between the blood and the red marrow residence times was assumed for estimating the red marrow radiation dose (18). The proportionality factor was the ratio between the red marrow mass and the blood mass in humans. OLINDA/EXM 1.0 was used to integrate the fitted time-activity curves and to estimate the organ and effective doses using the whole-body adult female model. For all calculations, the assumption was made that the mouse biodistribution, determined as the %IA/organ, was the same as the human biodistribution.

SPECT/CT Images

Mice were imaged using a nanoSPECT/CT system (Bioscan) 4 h after intravenous administration of 100 μL /5 MBq of ^{177}Lu -OPS201 (20, 200, and 2,000 pmol). A helical CT scan was acquired with the following parameters: current, 177 μA ; voltage, 45 kVp; pitch, 1. A helical SPECT scan was acquired using multipurpose pinhole collimators (APT1), 20% energy window width centered symmetrically over the 208- and 113-keV γ -peaks of ^{177}Lu , 24 projections, and 1,200 s per projection. CT and SPECT images were reconstructed and filtered using the manufacturer's algorithm, resulting in a pixel size of 0.3 mm for the SPECT and of 0.2 mm for the CT.

Data Analysis and Statistics

Mean and SD were used to describe normally distributed data. Bioequivalence regarding pharmacokinetics was assessed using area under the time-activity curve and residence time as estimated by the trapezoidal method for serial sacrifice (19), with the elimination rate after the last time point being equal to the isotope's physical decay. A comparison of biodistribution data was performed using the unpaired 2-tailed *t* test with GraphPad Prism 7 software. *P* values of less than 0.05 were considered significant.

RESULTS

Preparation of Radiotracers

^{177}Lu -OPS201 and ^{177}Lu -DOTATATE were prepared at specific activities of 23, 2.1, and 0.75 MBq/nmol for the biodistribution studies with 10, 200, and 2,000 pmol, respectively, and 250, 25, and 2.5 MBq/nmol for the SPECT/CT studies with 20, 200, and 2,000 pmol, respectively. ^{111}In -OPS201 and ^{90}Y -OPS201 were prepared at a specific activity of 29 and 25 MBq/nmol, respectively. The radiochemical yield was 95% or greater and radiochemical purity 93% or more for all preparations.

Biodistribution and Imaging Studies

Pharmacokinetics of ^{177}Lu -OPS201 and ^{177}Lu -DOTATATE. Table 1 presents the biodistribution results of 10 pmol ^{177}Lu -OPS201 and ^{177}Lu -DOTATATE at 4, 72, and 168 h. The entire biodistribution data from 1 to 168 h are presented in Supplemental Table 1 (supplemental materials are available at <http://jnm.snmjournals.org>). Both radiotracers are predominantly accumulated in SSTR2-expressing tumors and organs such as pancreas, stomach, and adrenals and have similar blood clearance (^{177}Lu -OPS201, 1.78 mL/h; ^{177}Lu -DOTATATE, 1.80 mL/h). The maximum tumor uptake was observed 4 h after injection for both radiotracers, with the antagonist showing the

TABLE 2
Biodistribution of 10 pmol ^{90}Y -OPS201 and ^{111}In -OPS201 in Nude Mice Bearing HEK-hsstr2 Tumor Xenografts

Organ	^{90}Y -OPS201			^{111}In -OPS201	
	4 h	24 h	72 h	4 h	72 h
Blood	0.07 ± 0.02	0.02 ± 0.00	0.01 ± 0.00	0.15 ± 0.02	0.00 ± 0.00
Heart	0.49 ± 0.15	0.12 ± 0.02	0.04 ± 0.01	0.22 ± 0.04	0.03 ± 0.00
Lung	8.81 ± 3.78	2.47 ± 0.43	1.38 ± 0.83	3.00 ± 1.45	0.32 ± 0.14
Liver	1.69 ± 0.50	0.72 ± 0.13	0.35 ± 0.11	0.64 ± 0.13	0.20 ± 0.02
Pancreas	46.3 ± 7.61	22.9 ± 1.70	5.18 ± 0.89	19.5 ± 4.29	0.93 ± 0.31
Spleen	0.98 ± 0.24	0.41 ± 0.08	0.31 ± 0.14	0.47 ± 0.08	0.16 ± 0.02
Stomach	46.1 ± 10.2	23.2 ± 2.56	9.83 ± 1.37	14.0 ± 1.73	1.53 ± 0.24
Intestine	11.2 ± 4.50	6.64 ± 0.52	2.50 ± 0.64	3.66 ± 1.78	0.57 ± 0.07
Adrenal	14.0 ± 2.26	7.21 ± 1.07	3.42 ± 0.75	3.62 ± 0.97	0.45 ± 0.10
Kidney	4.74 ± 1.07	4.31 ± 0.62	1.97 ± 0.35	7.29 ± 1.19	2.78 ± 0.40
Muscle	0.09 ± 0.06	0.04 ± 0.02	0.02 ± 0.01	0.09 ± 0.03	0.03 ± 0.01
Femur	1.09 ± 0.94	0.13 ± 0.11	0.20 ± 0.14	1.07 ± 0.75	0.14 ± 0.09
Salivary gland	2.39 ± 1.14	0.56 ± 0.07	0.19 ± 0.16	0.63 ± 0.31	0.06 ± 0.01
Tumor	17.9 ± 4.55	21.3 ± 7.86	7.41 ± 1.57	30.0 ± 4.56	12.8 ± 2.08

Data are %IA/g ± SD, *n* = 6–10.

TABLE 3

Biodistribution of ^{177}Lu -OPS201 and ^{177}Lu -DOTATATE 4 Hours After Injection in Nude Mice Bearing HEK-hsstr2 Tumor Xenografts: A Mass-Escalation Study

Organ	10 pmol	200 pmol	2,000 pmol
^{177}Lu-OPS201			
Blood	0.10 ± 0.02	0.03 ± 0.01	0.02 ± 0.01
Heart	0.61 ± 0.09	0.11 ± 0.03	0.04 ± 0.01
Lung	6.59 ± 3.41	1.34 ± 0.95	0.26 ± 0.04
Liver	1.45 ± 0.33	0.47 ± 0.15	0.24 ± 0.07
Pancreas	47.0 ± 4.20	10.7 ± 2.80	0.96 ± 0.45
Spleen	1.39 ± 0.69	0.25 ± 0.05	0.12 ± 0.03
Stomach	49.8 ± 8.19	7.55 ± 1.45	1.02 ± 0.14
Intestine	9.46 ± 2.24	1.96 ± 0.38	0.36 ± 0.10
Adrenal	8.16 ± 1.72	1.63 ± 0.64	0.38 ± 0.10
Kidney	5.88 ± 0.85	6.43 ± 1.60	6.23 ± 1.91
Muscle	0.10 ± 0.03	0.03 ± 0.01	0.03 ± 0.01
Femur	1.24 ± 0.92	0.31 ± 0.15	0.14 ± 0.03
Salivary gland	2.32 ± 0.47	0.36 ± 0.21	0.11 ± 0.02
Tumor	23.9 ± 4.76	24.9 ± 6.24*	18.8 ± 2.13†
^{177}Lu-DOTATATE			
Blood	0.07 ± 0.01	0.03 ± 0.02	0.02 ± 0.00
Heart	0.29 ± 0.06	0.06 ± 0.02	0.02 ± 0.00
Lung	6.54 ± 3.49	1.58 ± 0.90	0.19 ± 0.08
Liver	0.26 ± 0.04	0.13 ± 0.03	0.06 ± 0.01
Pancreas	10.3 ± 1.66	3.48 ± 1.77	0.40 ± 0.13
Spleen	0.76 ± 0.18	0.14 ± 0.03	0.05 ± 0.01
Stomach	12.2 ± 2.23	4.07 ± 1.05	0.53 ± 0.10
Intestine	5.80 ± 1.20	1.59 ± 0.30	0.24 ± 0.07
Adrenal	9.27 ± 2.49	2.32 ± 1.31	0.49 ± 0.05
Kidney	5.10 ± 0.94	4.02 ± 1.18	3.41 ± 0.17
Muscle	0.03 ± 0.01	0.02 ± 0.01	0.01 ± 0.00
Femur	1.55 ± 0.36	0.23 ± 0.18	0.06 ± 0.03
Salivary gland	0.68 ± 0.40	0.19 ± 0.16	0.04 ± 0.02
Tumor	17.8 ± 4.35	12.0 ± 2.16‡	9.94 ± 2.52¶

* $P = 0.7948$, compared with 10 pmol ^{177}Lu -OPS201.

† $P = 0.0813$, compared with 10 pmol ^{177}Lu -OPS201.

‡ $P = 0.0450$, compared with 10 pmol ^{177}Lu -DOTATATE.

¶ $P = 0.0249$, compared with 10 pmol ^{177}Lu -DOTATATE.

Data are %IA/g ± SD, $n = 3-6$.

highest uptake ($P = 0.044$). The maximum renal uptake was found 1 h after injection for ^{177}Lu -OPS201 and at 4 h after injection for ^{177}Lu -DOTATATE. The SSTR2 specificity of both radiotracers was confirmed in vivo by blockage experiments (Supplemental Table 2).

Figure 1 shows the time-activity curve in HEK-hsstr2 tumor for ^{177}Lu -OPS201 and ^{177}Lu -DOTATATE. The mean tumor residence time was 15.6 h (95% confidence interval, 13.4–17.7) for the antagonist and 6.4 h (95% confidence interval, 5.4–7.3) for the agonist, based on non-decay-corrected biodistribution data and normalized per gram of tumor.

Influence of Radiometal (^{177}Lu , ^{90}Y , and ^{111}In) on Biodistribution of OPS201. The biodistribution results of 10 pmol ^{90}Y -OPS201

and ^{111}In -OPS201 are presented in Table 2 and compared with ^{177}Lu -OPS201 (Table 1). ^{90}Y -OPS201 had distribution and pharmacokinetic profile similar to those of ^{177}Lu -OPS201. On the contrary, the uptake of ^{111}In -OPS201 in all SSTR-expressing tissues was significantly lower than ^{177}Lu -OPS201 and ^{90}Y -OPS201, at 4 and 72 h. In comparison to ^{90}Y -OPS201, the uptake of ^{111}In -OPS201 was significantly higher in the tumor ($P < 0.0001$ [4 h] and $P = 0.0005$ [72 h]) and in the kidneys ($P < 0.0001$ [4 h] and $P = 0.004$ [72 h]) at both time points.

Effect of Mass Escalation on Biodistribution. Escalation of the administered amount of ^{177}Lu -OPS201 from 10 to 200 and 2,000 pmol showed no relevant saturation in the tumor 4 h after injection (Table 3). By contrast, this increase greatly suppressed the uptake in all SSTR-expressing organs and other tissues and consequently enhanced the tumor-to-background ratios (Supplemental Table 3). Similarly for ^{177}Lu -DOTATATE, increased mass reduced the background activity; however, it also saturated the tumor uptake (Table 3). In both cases, the tumor-to-kidney dose ratio remained essentially the same. The mass effect was demonstrated on nanoSPECT/CT images acquired 4 h after injection of 20, 200, and 2,000 pmol ^{177}Lu -OPS201 (Fig. 2), showing clear improvement of the image contrast along the mass escalation.

Effects of Mass Escalation on Pharmacokinetics. The pharmacokinetics of 200 pmol of ^{177}Lu -OPS201 and ^{177}Lu -DOTATATE are shown in Supplemental Table 4. Over time, the tumor uptake and retention remained at the same level for 10 and 200 pmol ^{177}Lu -OPS201, with a mean tumor residence time of 13.3 h (95% confidence interval, 8.81–17.8) for 200 pmol. Tumor-to-nontumor ratios were impressively increased due to the substantial reduction in background activity. When the agonist and the antagonist were compared, similar observations were made with 200 pmol as with 10 pmol.

Nephroprotective Agents. The kidney uptake of 10 pmol ^{177}Lu -OPS201 at 4 h was reduced by 45%, 25%, and 40% when lysine, Gelifusine, and a combination of both were used (from 5.88 ± 0.85 to 3.23 ± 0.63 %IA/g [$P < 0.0001$], 4.45 ± 0.55 %IA/g

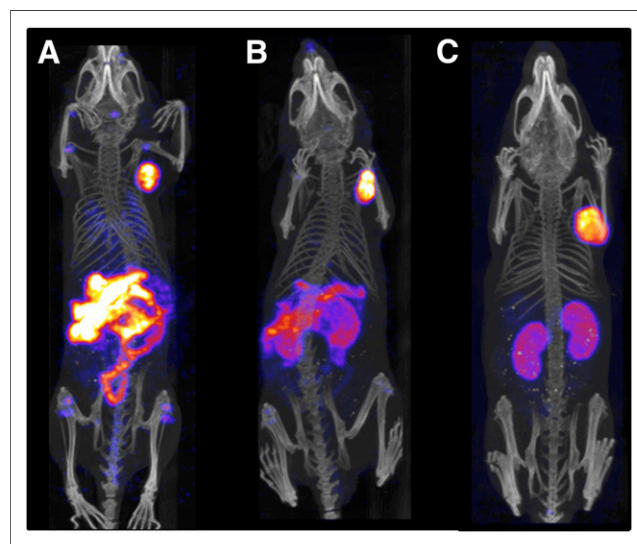


FIGURE 2. nanoSPECT/CT images of HEK-hsstr2 xenografts 4 h after administration of 20 pmol (A), 200 pmol (B), and 2,000 pmol (C) of ^{177}Lu -OPS201.

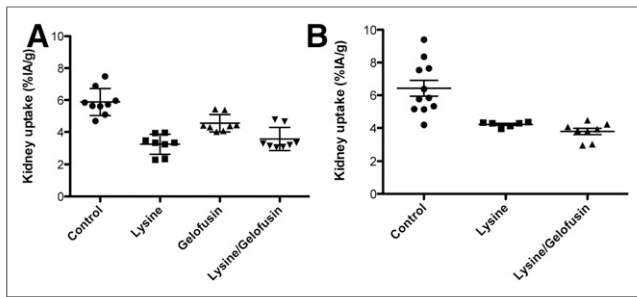


FIGURE 3. Kidney uptake of 10 pmol ^{177}Lu -OPS201 (A) and 200 pmol ^{177}Lu -OPS201 (B) in HEK-hsst2 xenografts at 4 h after injection, without (control) and with 3–5 min preinjection of lysine, Gelofusine, and lysine–Gelofusine as kidney-protecting agents. A significant reduction of the kidney uptake was found with all agents compared with the control group ($P < 0.05$), with lysine or combination of lysine–Gelofusine being better than Gelofusine alone ($P < 0.05$).

[$P = 0.0018$], and 3.56 ± 0.72 %IA/g [$P < 0.0001$], respectively) (Fig. 3A). Among the protecting agents, lysine and the combination of lysine–Gelofusine performed better, resulting in a significantly lower kidney uptake than Gelofusine alone ($P < 0.05$). Therefore, these 2 schemes were also evaluated after administration of 200 pmol ^{177}Lu -OPS201, leading to similar kidney uptake reduction (Fig. 3B).

Dosimetry

Table 4 shows the radiation dose estimate for human organs and tumors after injection of 10 pmol ^{177}Lu -OPS201, ^{90}Y -OPS201, and ^{177}Lu -DOTATATE, based on a female phantom. The tumor dose was calculated for tumors with a diameter of 4 cm to estimate the therapeutic index, defined as the tumor–to–critical organ dose ratios (Table 4). The estimated whole-body radiation dose (effective dose) was 0.0908 mSv/MBq for ^{177}Lu -OPS201, almost 5-times lower than ^{90}Y -OPS201 (0.431 mSv/MBq) and 2.9-times higher than ^{177}Lu -DOTATATE (0.0317 mSv/MBq). ^{177}Lu -OPS201, compared with ^{90}Y -OPS201, delivered about a 3.2-fold-lower tumor dose, but had a 24% higher tumor–to–kidney dose ratio. ^{177}Lu -OPS201, compared with ^{177}Lu -DOTATATE, delivered a 2.6-fold-higher tumor dose and it also had a 32% higher tumor–to–kidney dose ratio. The effective dose delivered by the antagonist was drastically reduced when a higher peptide mass of 200 pmol was used. When 200 pmol ^{177}Lu -OPS201 was compared with 10 pmol ^{177}Lu -OPS201 and ^{177}Lu -DOTATATE, the effective dose was reduced by 80% and 42%, respectively (0.0184 vs. 0.0908 and 0.0317 mSv/MBq), the tumor–to–kidney dose ratio remained at the same level, whereas importantly, the tumor dose remained 2.3-fold higher for the antagonist versus the agonist.

DISCUSSION

Two crucial parameters for a therapeutic radiotracer are its prolonged residence time on the molecular target (15) combined with a fast clearance from critical (nontarget) organs. We showed in a xenograft model that the antagonist ^{177}Lu -OPS201 had a moderately higher tumor uptake but, most importantly, significantly longer tumor retention, resulting in an approximately 2.5-times-higher absorbed tumor dose than the agonist ^{177}Lu -DOTATATE. This is in line with our first-in-human data (13) and also with the results in another SSTR2 xenograft model (20). Although the antagonist showed higher kidney uptake, the

tumor–to–kidney dose ratio, thus the therapeutic index, remained in favor of the antagonist by 32%. Dalm et al. reported a kidney uptake of ^{177}Lu -OPS201 in a BALB/c nude mouse model of 30 % IA/g, 4 h after injection (20). We have not observed such high renal uptake in this or any of our previous studies with JR11, using different chelating systems and radionuclides (17). Therefore, we do not confirm such a high renal uptake for this radiotracer.

Recent works investigating the occurrence of renal toxicity after ^{177}Lu -DOTATATE therapy (21,22) have found low frequency of severe kidney toxicity after ^{177}Lu -based PRRT, therefore questioning the dogma that kidneys are the critical organs in this type of therapy. On the other hand, hematologic toxicity may be a dose-limiting factor. In our study, the tumor–to–bone marrow dose ratio was in favor of ^{177}Lu -OPS201 by a factor of 1.7 compared with ^{177}Lu -DOTATATE (10 pmol). Nonetheless, we noticed a 49% higher bone marrow dose and 2.9-fold-higher effective dose for ^{177}Lu -OPS201, than ^{177}Lu -DOTATATE, at this mass level. Increasing the mass from 10 to 200 pmol drastically reduced the absorbed dose in nontarget organs as well as the effective dose, with essentially no influence on the tumor dose. Tumor–to–bone marrow and tumor–to–spleen dose ratios increased by at least a factor of 2.4, which should be beneficial in terms of hematologic toxicity. In addition, the tumor-to-liver ratio, the main organ of distant metastases in NET, is improved by a factor of 2.1. Conversely, the tumor-to-kidney ratio remained the same, independently of the injected peptide amount. At 4 h after injection, and as clearly illustrated by the improved imaging contrast on nanoSPECT/CT images, relevant tumor-to-organ ratios, such as tumor-to-pancreas, -intestine, or -liver (sites of primary or distant metastases in gastro-entero-pancreatic-NET), increased considerably with higher peptide amounts. This is of great value from a theranostic point of view.

The striking sensitivity of the SSTR antagonists to any modifications of the chelates (16,17) necessitates the evaluation of ^{90}Y -OPS201 as another possible therapeutic tracer and of ^{111}In -OPS201 as a theranostic companion. Indeed, ^{111}In is often used as a surrogate for ^{90}Y to perform imaging and dosimetry. ^{111}In -OPS201, having 8 times lower affinity for SSTR2 than ^{90}Y -OPS201 (half maximal inhibitory concentration, 3.8 ± 0.7 vs. 0.47 ± 0.05 nM (17)), showed significant differences in the biodistribution profile. Therefore, it is not recommended to use ^{111}In -OPS201 as a surrogate for ^{90}Y -OPS201. Nevertheless, ^{111}In -OPS201 may be an excellent SPECT tracer for imaging SSTR2 in vivo.

^{177}Lu -OPS201 and ^{90}Y -OPS201 have similar affinity for the SSTR2 (half maximal inhibitory concentration, 0.73 ± 0.15 and 0.47 ± 0.05 nM, respectively (17)), reflecting their similar in vivo profiles. ^{90}Y -OPS201 delivers with a higher dose rate a higher tumor dose, due to the higher energy of its β^- particles. On the other hand, the longer half-life of ^{177}Lu (161.5 h; ^{90}Y half-life, 64 h) may be a better match for the longer tumor retention of OPS201. In addition, the dose ratio of ^{177}Lu versus ^{90}Y increases as the radius of the tumor decreases (23). For comparison, we estimated the absorbed doses of ^{177}Lu -OPS201 and ^{90}Y -OPS201 in tumors of 4 cm; as for smaller tumors (<1 cm), the dose distribution is largely dependent on the particle range. The 5-times-lower effective dose together with the 24% higher tumor–to–kidney dose ratio of ^{177}Lu -OPS201 may favor ^{177}Lu - over ^{90}Y -OPS201 for PRRT in NETs. Our studies also suggest that because the highest tumor uptake for ^{177}Lu -OPS201 was observed 4 h after injection and the optimum tumor-to-organ ratios were obtained at even later time points, the use of long-lived isotopes

TABLE 4

Radiation Dose Estimation, Extrapolated from Mice to Humans and Expressed as Mean Absorbed Dose (mGy/MBq), for ^{177}Lu -OPS201, ^{90}Y -OPS201, and ^{177}Lu -DOTATATE

Organ/tissue	^{177}Lu -OPS201 (10 pmol)	^{90}Y -OPS201 (10 pmol)	^{177}Lu -DOTATATE (10 pmol)	^{177}Lu -OPS201 (200 pmol)
Adrenals	2.03E-01	9.71E-01	2.37E-01	3.79E-02
Intestine	3.79E-01	2.44E+00	3.38E-01	1.06E-01
Stomach	3.97E-01	1.64E+00	1.27E-01	6.19E-02
Heart	8.73E-03	2.83E-02	6.44E-03	2.48E-03
Kidneys	4.14E-01	1.72E+00	2.13E-01	4.06E-01
Liver	4.09E-02	1.78E-01	1.16E-02	1.67E-02
Lungs	2.45E-02	1.24E-01	4.07E-02	6.11E-03
Muscle	1.19E-03	0.00E+00	6.94E-04	4.05E-04
Pancreas	1.36E+00	7.88E+00	3.10E-01	3.00E-01
Red marrow	1.87E-03	1.29E-03	1.25E-03	6.63E-04
Spleen	4.71E-02	1.48E-01	3.13E-02	1.53E-02
Salivary glands	4.01E-01	1.78E+00	9.13E-02	6.58E-02
Total body	1.16E-02	5.81E-02	7.04E-03	4.60E-03
Tumor (diameter, 4 cm)	8.54E-01	2.85E+00	3.33E-01	7.50E-01
Effective dose (mSv/MBq)	9.08E-02	4.31E-01	3.17E-02	1.84E-02
Tumor-to-organ ratio				
Tumor to kidney	2.06	1.66	1.56	1.85
Tumor to bone marrow	457	2,209	266	1,131
Tumor to spleen	18.1	19.3	10.6	49.0
Tumor to liver	20.9	16.0	28.7	44.9

for imaging and theranostic application, such as ^{64}Cu , may be of interest over the short-lived isotope ^{68}Ga .

Different peptide amounts or specific activities have previously been tested in animal models and in humans to attempt to influence the biodistribution of radiolabeled SSTR agonists (24–27). However, data regarding the effect of the amount of radiolabeled SSTR antagonist are scarce. Currently, a relatively low peptide amount of 50 μg or less for imaging (28) and 200 μg or less for PRRT with ^{90}Y - ^{177}Lu -DOTATOC or ^{177}Lu -DOTATATE is used clinically (29) to avoid the risk of receptor saturation on a rather limited number of available receptor binding sites on tumors. However, these amounts are more reflective of common practice than of evidence from controlled studies. We systematically addressed the issue of escalation of administered amount of antagonist, using 10, 200, and 2,000 pmol, and compared it with agonists. This showed that 1-to-1 translation from agonist to antagonist should be avoided and that greater peptide mass could be preferable (e.g., 200–2,000 pmol vs. 10 pmol) for the antagonists. Translation from mice-to-human equivalent dose is rather complex but, considering several models, including body weight-based allometric scaling, 200 pmol may represent a peptide amount higher than 200 μg up to 1,300 μg in human. This indicates that the upper limit of 200 μg or less for the agonists might represent a starting dose for the antagonists, to overcome potential drawbacks. We focused on the 200-pmol dose, because an amount of 2,000 pmol, which would correspond to more than 2 mg in humans, is more likely to cause pharmacologic effect and growth hormone release (30).

CONCLUSION

^{177}Lu -OPS201 exhibits a higher tumor uptake, a longer tumor residence time, and an improved tumor-to-kidney dose ratio compared with ^{177}Lu -DOTATATE and ^{90}Y -OPS201. Because of the long tumor residence time, lower effective dose, and improved tumor-to-kidney dose ratio, the use of ^{177}Lu may be preferable over ^{90}Y , whereas ^{111}In should not be used as a surrogate for ^{90}Y for this specific radiotracer. Known nephroprotective agents, especially lysine, are recommended during PRRT with ^{177}Lu -OPS201. Importantly, the mass-escalation study indicates that an optimized amount of antagonist might further improve the safety window of PRRT by reducing bone marrow, liver, and also the effective dose of ^{177}Lu -OPS201. Clinical studies are warranted to confirm the efficacy and advantageous toxicity profile of ^{177}Lu -OPS201.

DISCLOSURE

Financial support for this work was provided with OctreoPharm/Ipsen. Hakim Bouterfa and Jens Kaufmann are employees of Ipsen. No other potential conflict of interest relevant to this article was reported.

ACKNOWLEDGMENTS

We thank Prof. Stefan Schulz for the HEK-hsstr2-transfected cells, Sandra Vomstein MSc and Rudolf von Wartburg for their support in conducting animal experiments, and ITM (Munich, Germany) for kindly providing $^{177}\text{LuCl}_3$.

REFERENCES

1. Yao JC, Hassan M, Phan A, et al. One hundred years after "carcinoid": epidemiology of and prognostic factors for neuroendocrine tumors in 35,825 cases in the United States. *J Clin Oncol*. 2008;26:3063–3072.
2. Modlin IM, Oberg K, Chung DC, et al. Gastroenteropancreatic neuroendocrine tumours. *Lancet Oncol*. 2008;9:61–72.
3. Frilling A, Modlin IM, Kidd M, et al. Recommendations for management of patients with neuroendocrine liver metastases. *Lancet Oncol*. 2014;15:e8–e21.
4. van Essen M, Krenning EP, Kam BL, de Jong M, Valkema R, Kwekkeboom DJ. Peptide-receptor radionuclide therapy for endocrine tumors. *Nat Rev Endocrinol*. 2009;5:382–393.
5. Ambrosini V, Fani M, Fanti S, Forrer F, Maecke HR. Radiopeptide imaging and therapy in Europe. *J Nucl Med*. 2011;52(suppl 2):42S–55S.
6. Imhof A, Brunner P, Marincek N, et al. Response, survival, and long-term toxicity after therapy with the radiolabeled somatostatin analogue [⁹⁰Y-DOTA]-TOC in metastasized neuroendocrine cancers. *J Clin Oncol*. 2011;29:2416–2423.
7. Kwekkeboom DJ, de Herder WW, Kam BL, et al. Treatment with the radiolabeled somatostatin analog [¹⁷⁷Lu-DOTA⁰,Tyr³]octreotate: toxicity, efficacy, and survival. *J Clin Oncol*. 2008;26:2124–2130.
8. Bodei L, Kwekkeboom DJ, Kidd M, Modlin IM, Krenning EP. Radiolabeled somatostatin analogue therapy of gastroenteropancreatic cancer. *Semin Nucl Med*. 2016;46:225–238.
9. Ginj M, Zhang H, Waser B, et al. Radiolabeled somatostatin receptor antagonists are preferable to agonists for in vivo peptide receptor targeting of tumors. *Proc Natl Acad Sci USA*. 2006;103:16436–16441.
10. Cascato R, Waser B, Fani M, Reubi JC. Evaluation of ¹⁷⁷Lu-DOTA-sst2 antagonist versus ¹⁷⁷Lu-DOTA-sst2 agonist binding in human cancers in vitro. *J Nucl Med*. 2011;52:1886–1890.
11. Wild D, Fani M, Behe M, et al. First clinical evidence that imaging with somatostatin receptor antagonists is feasible. *J Nucl Med*. 2011;52:1412–1417.
12. Cascato R, Ercegyi J, Waser B, et al. Design and in vitro characterization of highly sst2-selective somatostatin antagonists suitable for radiotargeting. *J Med Chem*. 2008;51:4030–4037.
13. Wild D, Fani M, Fischer R, et al. Comparison of somatostatin receptor agonist and antagonist for peptide receptor radionuclide therapy: a pilot study. *J Nucl Med*. 2014;55:1248–1252.
14. Reubi JC, Waser B, Macke H, Rivier J. Highly increased ¹²⁵I-JR11 antagonist binding in vitro reveals novel indications for sst2 targeting in human cancers. *J Nucl Med*. 2017;58:300–306.
15. Copeland RA, Pompliano DL, Meek TD. Drug-target residence time and its implications for lead optimization. *Nat Rev Drug Discov*. 2006;5:730–739.
16. Fani M, Del Pozzo L, Abiraj K, et al. PET of somatostatin receptor-positive tumors using ⁶⁴Cu- and ⁶⁸Ga-somatostatin antagonists: the chelate makes the difference. *J Nucl Med*. 2011;52:1110–1118.
17. Fani M, Braun F, Waser B, et al. Unexpected sensitivity of sst2 antagonists to N-terminal radiometal modifications. *J Nucl Med*. 2012;53:1481–1489.
18. Sgouros G. Bone marrow dosimetry for radioimmunotherapy: theoretical considerations. *J Nucl Med*. 1993;34:689–694.
19. Wolfsegger MJ, Jaki T. Estimation of AUC from 0 to Infinity in serial sacrifice designs. *J Pharmacokinetic Pharmacodyn*. 2005;32:757–766.
20. Dalm SU, Nonnekens J, Doeswijk GN, et al. Comparison of the therapeutic response to treatment with a ¹⁷⁷Lu-labeled somatostatin receptor agonist and antagonist in preclinical models. *J Nucl Med*. 2016;57:260–265.
21. Sabet A, Ezziddin K, Pape UF, et al. Accurate assessment of long-term nephrotoxicity after peptide receptor radionuclide therapy with ¹⁷⁷Lu-octreotate. *Eur J Nucl Med Mol Imaging*. 2014;41:505–510.
22. Strosberg J, El-Haddad G, Wolin E, et al. Phase 3 trial of ¹⁷⁷Lu-Dotatate for midgut neuroendocrine tumors. *N Engl J Med*. 2017;376:125–135.
23. Siegel JA, Stabin MG. Absorbed fractions for electrons and beta particles in spheres of various sizes. *J Nucl Med*. 1994;35:152–156.
24. Breeman WA, Kwekkeboom DJ, Kooij PP, et al. Effect of dose and specific activity on tissue distribution of indium-111-pentetreotide in rats. *J Nucl Med*. 1995;36:623–627.
25. de Jong M, Breeman WA, Bernard BF, et al. Tumour uptake of the radiolabelled somatostatin analogue [DOTA⁰, TYR³]octreotide is dependent on the peptide amount. *Eur J Nucl Med*. 1999;26:693–698.
26. Bernhardt P, Kolby L, Johanson V, Nilsson O, Ahlman H, Forsell-Aronsson E. Biodistribution of ¹¹¹In-DTPA-D-Phe¹-octreotide in tumor-bearing nude mice: influence of amount injected and route of administration. *Nucl Med Biol*. 2003;30:253–260.
27. Velikyan I, Sundin A, Eriksson B, et al. In vivo binding of [⁶⁸Ga]-DOTATOC to somatostatin receptors in neuroendocrine tumours—impact of peptide mass. *Nucl Med Biol*. 2010;37:265–275.
28. Virgolini I, Ambrosini V, Bomanji JB, et al. Procedure guidelines for PET/CT tumour imaging with ⁶⁸Ga-DOTA-conjugated peptides: ⁶⁸Ga-DOTA-TOC, ⁶⁸Ga-DOTA-NOC, ⁶⁸Ga-DOTA-TATE. *Eur J Nucl Med Mol Imaging*. 2010;37:2004–2010.
29. Bodei L, Mueller-Brand J, Baum RP, et al. The joint IAEA, EANM, and SNMMI practical guidance on peptide receptor radionuclide therapy (PRRT) in neuroendocrine tumours. *Eur J Nucl Med Mol Imaging*. 2013;40:800–816.
30. Tulipano G, Soldi D, Bagnasco M, et al. Characterization of new selective somatostatin receptor subtype-2 (sst2) antagonists, BIM-23627 and BIM-23454: effects of BIM-23627 on GH release in anesthetized male rats after short-term high-dose dexamethasone treatment. *Endocrinology*. 2002;143:1218–1224.